LETTERS

Weakening of tropical Pacific atmospheric circulation due to anthropogenic forcing

Gabriel A. Vecchi[1], Brian J. Soden[2], Andrew T. Wittenberg[1], Isaac M. Held[1], Ants Leetmaa[1] & Matthew J. Harrison[1]

Since the mid-nineteenth century the Earth's surface has warmed[1–3], and models indicate that human activities have caused part of the warming by altering the radiative balance of the atmosphere[1,3]. Simple theories suggest that global warming will reduce the strength of the mean tropical atmospheric circulation[4,5]. An important aspect of this tropical circulation is a large-scale zonal (east–west) overturning of air across the equatorial Pacific Ocean—driven by convection to the west and subsidence to the east—known as the Walker circulation[6]. Here we explore changes in tropical Pacific circulation since the mid-nineteenth century using observations and a suite of global climate model experiments. Observed Indo-Pacific sea level pressure reveals a weakening of the Walker circulation. The size of this trend is consistent with theoretical predictions, is accurately reproduced by climate model simulations and, within the climate models, is largely due to anthropogenic forcing. The climate model indicates that the weakened surface winds have altered the thermal structure and circulation of the tropical Pacific Ocean. These results support model projections of further weakening of tropical atmospheric circulation during the twenty-first century[4,5,7].

The Walker circulation is fundamental to climate throughout the globe: its variations are closely linked to those of the El Niño/Southern Oscillation[6] and monsoonal circulations over adjacent continents[8], and variations in its intensity and structure affect climate across the planet[8,9]. The strength of equatorial Pacific zonal wind-stress, associated with the Walker circulation, is critical to equatorial Pacific Ocean circulation[10] and to biogeochemical processes[11].

Observational and modelling evidence indicates that since the mid-nineteenth century tropical sea surface temperatures (SSTs) have warmed by 0.5–0.6 °C (refs 1–3). Climate models predict a weakening of the atmospheric convective overturning in response to surface warming driven by increases in greenhouse gases[4,5,7]. One expects this weakening to be manifest, in part, as a reduction in the zonal overturning of tropical air[4], a large component of which is the Pacific Walker circulation[6].

The weakening of tropical atmospheric overturning circulations in response to warming can be understood in terms of the energy and mass balance of the ascending branch of these circulations. As the surface warms, the water vapour concentration in the lower troposphere increases by roughly 7% per °C of surface warming[12,13], consistent with the Clausius–Clapeyron equation and fixed relative humidity. However, the rate of precipitation (which on long timescales is limited by the rate of change of the radiative cooling of the troposphere) increases more slowly—approximately 2% per °C warming[1,14,15]. The global-mean rate of precipitation must be balanced by the moisture transport from the atmospheric boundary layer to the free troposphere, which is a product of the boundary layer water vapour concentration and the exchange of air between the boundary layer and free troposphere. Thus, the differential rate of response to surface warming of water vapour and precipitation

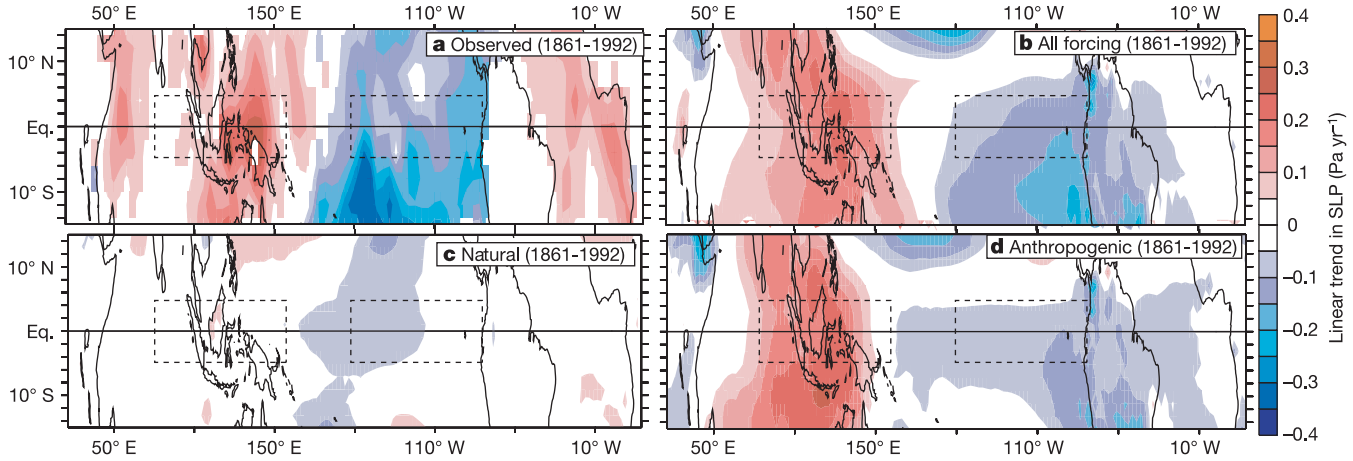

Figure 1 | Spatial pattern of observed and modelled sea level pressure linear trends. Linear trend of sea level pressure (SLP) from: **a**, Kaplan SLP reconstruction[29] (1861–1992), and ensemble-mean of GCM experiments (1861–1992) as follows; **b**, all-forcing (five-member mean), **c**, natural forcing (three-member mean) and **d**, anthropogenic forcing (three-member mean). The trend averaged over the domain 15° S–15° N, 0°–360° is removed from each panel. Dashed rectangles indicate the regions used to define the large-scale Indo-Pacific SLP gradient index (ΔSLP).

[1]NOAA/Geophysical Fluid Dynamics Laboratory, Princeton, New Jersey 08540-6649, USA. [2]Rosenstiel School for Marine and Atmospheric Sciences, University of Miami, Miami, Florida 33149-1098, USA.

implies a weakening of the boundary layer/troposphere mass exchange of ~5% per °C warming[4]. Closely related arguments have been provided for a weakening of tropical overturning circulations based on the energy balance of the subsiding branch of these circulations[5]. On the basis of observed tropical warming since the mid-nineteenth century (0.5–0.6 °C), these theoretical arguments predict a 2.5–3% reduction in the strength of tropical atmospheric overturning circulation. Is there evidence of such a slowdown in the observational record?

We use historical observations of sea level pressure (SLP) to assess observed changes in the Walker circulation over the tropical Pacific; an index of the large-scale tropical Indo-Pacific SLP gradient (ΔSLP) serves as a proxy for the mean intensity of the Pacific Walker circulation (see Methods). Ensembles of global climate model (GCM) experiments—with different radiative forcings—serve to explore the origin of the observed circulation changes, and allow for the estimation of the statistical significance of the observed changes. The model used here is the US National Oceanic and Atmospheric Administration (NOAA) Geophysical Fluid Dynamics Laboratory (GFDL) CM2.1 GCM[16–18], with three historical integration sets over the period 1861–2000: (1) a five-member ensemble including estimates of natural (solar variations, volcanoes) and anthropogenic (well-mixed greenhouse gases, ozone, direct aerosol forcing and land use) sources of climate change; (2) a three-member ensemble applying only natural forcing; and (3) a three-member ensemble applying only anthropogenic forcing (see Methods and Supplementary Information).

There have been spatially coherent patterns in observed trends of tropical SLP since the mid-nineteenth century (Fig. 1a), and similar patterns are evident in the five-member ensemble-mean of the historically forced GCM integrations (Fig. 1b). These trends indicate a reduced zonal SLP gradient, and thus a weakened zonal circulation, because the climatological pattern in the tropical Indo-Pacific has SLP larger in the east than in the west. The naturally forced GCM experiments are unable to recover these observed patterns in the SLP trends (Fig. 1c); however, the GCM recovers many of the principal observed SLP trend patterns using only anthropogenic forcing (Fig. 1d).

Trends computed from observed ΔSLP are inconsistent with those expected from the variability in the pre-industrial control simulation, and they are inconsistent with the trends from the 'natural-forcing' GCM ensemble experiment (Fig. 2). However, the trends in observed ΔSLP fall within the range of trends from the 'all-forcing' GCM ensemble, and within that of the 'anthropogenic-forcing' GCM ensemble (Fig. 2). Thus, within the framework of this GCM, a significant part of the observed reduction of ΔSLP since the mid-nineteenth century resulted from anthropogenic forcing. The trend computed from observed ΔSLP is also significantly distinct from that expected from the pre-industrial control experiments of all other models in the Intergovernmental Panel on Climate Change 4th Assessment Report (IPCC/AR4) archive (Supplementary Fig. 3). Most other models in the IPCC/AR4 archive also show a weakening of the equatorial Pacific pressure gradient, although CM2.1 shows the largest reduction (Supplementary Fig. 4.)

Though we use linear trends to summarize the changes in tropical SLP since the mid-nineteenth century, these changes have not appeared as a smooth reduction (Fig. 3). Both the observational record and individual GCM ensemble members exhibit substantial decadal variability (Supplementary Fig. 1), arising from processes internal to the coupled system. The GCM decadal variability in ΔSLP is comparable to that in observations, even though the GCM interannual variability is overly energetic owing to a simulated El Niño variability that has too large an amplitude[17]. The strong decadal variability complicates the detection of a relatively small forced change even in multi-decadal records of ΔSLP; on the basis of the 2,000-year control integration, a record shorter than 100–120 years is insufficient to detect the forced linear trend in ΔSLP from the GCM at $P = 0.05$ (Supplementary Fig. 2).

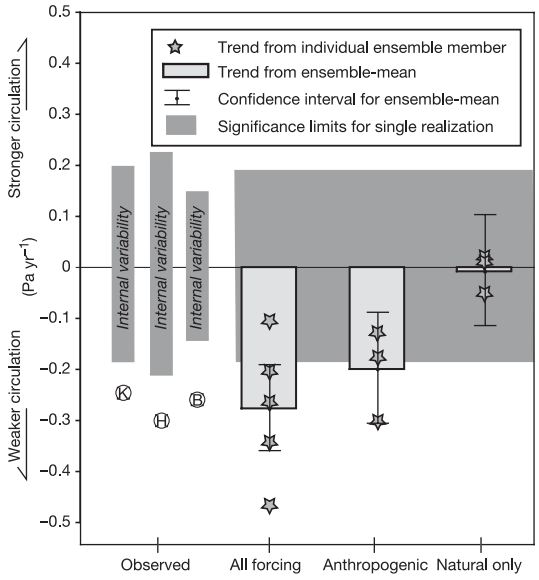

Figure 2 | Summary of the linear trends in SLP gradient across the Indo-Pacific (ΔSLP) from observations and the various GCM historical radiative forcing experiments. Circles indicate the trend value from each observational data set: K, Kaplan (1854–1992)[29]; H, Hadley Centre (1871–1998)[28]; and B, a blend of Hadley[28] and Kaplan[29], extended into 2005 using the NCEP gridded ship data (1854–2005)[27]. Model trends are computed over the period 1861–2000. Confidence intervals are computed from a 2,000-year control experiment, at the two-sided $P = 0.05$ level.

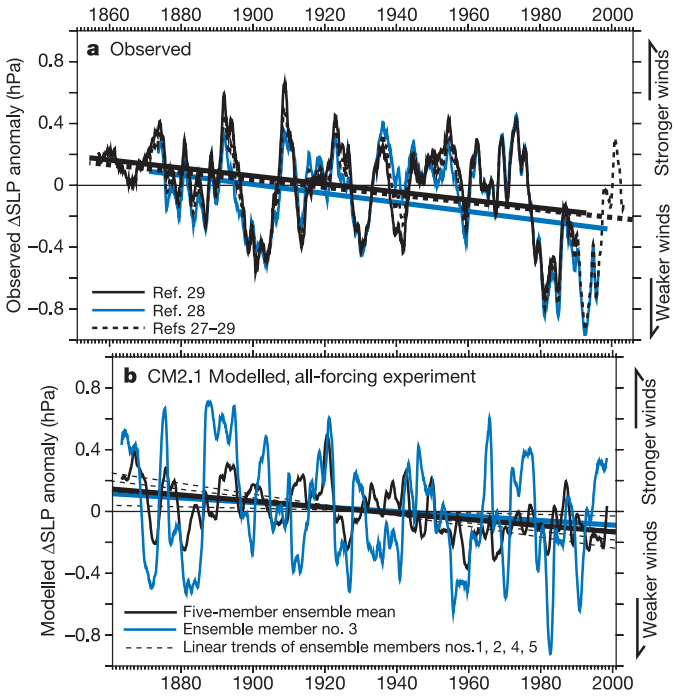

Figure 3 | Observed and modelled evolution of ΔSLP since the nineteenth century. Five-year running-mean ΔSLP from: **a**, observations (black from Kaplan[29], and blue from Hadley Centre[28]; the record is extended through to 2005 with NCEP ship-based observations[27] (dashed line)); and **b**, GCM historical integrations (five-member ensemble mean in black, an illustrative ensemble member (number 3) in blue, dashed lines indicate linear trend of ensemble members 1, 2, 4 and 5). In both panels, the linear trends in ΔSLP are shown as thick lines, with shadings corresponding to each time-series.

In the 1970s there was a rapid reduction in observed ΔSLP; such rapid changes are also evident in other decades and in individual ensemble members. Fifty-year ΔSLP trends ending in the 1990s are significantly larger than those computed over the entire record, suggesting an amplifying trend in ΔSLP. However, in recent years the statistical significance of the amplification of the trend disappears; though nominally larger than the long-term trend, the 1956–2005 trend is not significantly different from the long-term trend at $P = 0.05$. Further work is required to determine if the larger recent trend since the 1950s is forced or a result of internal variability.

We estimate zonal wind stress across the equatorial Pacific using ΔSLP, following the method of ref. 19 (Fig. 4). Linear relationships with ΔSLP capture most of the interannual and longer timescale variability in equatorial Pacific zonal-mean easterlies ($<\tau^x>$; zonal wind-stress averaged 120° E–70° W, 5° S–5° N; easterlies are winds from the east). ΔSLP-reconstructed $<\tau^x>$ recovers the principal extremes and transitions of the observed and modelled $<\tau^x>$, including the long-term weakening of $<\tau^x>$ in the model, and the various El Niño and La Niña events observed in the recent decades (Fig. 4, upper panels). The trend of the linear fit of $<\tau^x>$ to observed ΔSLP represents a $<\tau^x>$ reduction of ~7% since 1860; as surface stress is roughly proportional to the square of wind speed, this suggests a mean reduction in equatorial Pacific zonal wind of ~3.5%, roughly consistent with the theoretical prediction.

Equatorial Pacific $<\tau^x>$ is of critical importance to the large-scale oceanic circulation in the equatorial Pacific[9]. The GCM experiments indicate that since the mid-nineteenth century, the weakening of equatorial $<\tau^x>$ has resulted in a weakening of surface equatorial currents, a vertical shift in sub-surface currents, and a reduction in the intensity and depth of equatorial upwelling (Supplementary Fig. 5). By bringing nutrient-rich waters close to the surface, equatorial upwelling exerts a strong control on biological activity in the tropical Pacific[10]; its weakening and shoaling suggest a possible reduction of biological productivity under global warming.

The GCM experiments indicate a substantial shoaling of the western equatorial Pacific thermocline depth (Z_{tc}) since the mid-nineteenth century (Fig. 4, lower panels); the thermocline is the zone of rapid temperature change in a typical vertical oceanic temperature profile between the warm well-mixed surface layer and cold abyssal waters. Reduction of $<\tau^x>$ affects both the east–west tilt of the equatorial Pacific thermocline and its mean depth[20] (Supplementary Fig. 6); these changes could affect the character of El Niño variability[21]. On seasonal to interannual timescales (timescales too short for the equatorial thermocline to come to equilibrium with the winds), a reduction in $<\tau^x>$ has a strong impact on both western and eastern equatorial Pacific Z_{tc}. However, on timescales longer than that of equatorial adjustment, the impact of reductions in $<\tau^x>$ is felt almost entirely by the western equatorial Pacific Z_{tc} (Fig. 4). Because Z_{tc} and SST are tightly coupled only in the eastern equatorial Pacific[22], these long-term thermocline depth changes in the GCM are unlikely to affect SST directly. The observational record of equatorial Pacific thermocline slope and depth over the past 50 years is consistent with the recent reduction in the strength of the easterlies and the low-frequency relationship between Z_{tc} and $<\tau^x>$ in the GCM.

Atmosphere–ocean conditions in the equatorial Pacific have changed since the mid-nineteenth century: there has been a significant slowdown of atmospheric circulation, which models indicate has driven a response in ocean circulation. The observed trend in the Pacific surface zonal SLP gradient is unlikely to be due to natural variability. However, much of the long-term trend is reproduced in model simulations that account for human impacts on the radiative budget of the planet, and is consistent with the changes expected from simple thermodynamic arguments[4]. The agreement between

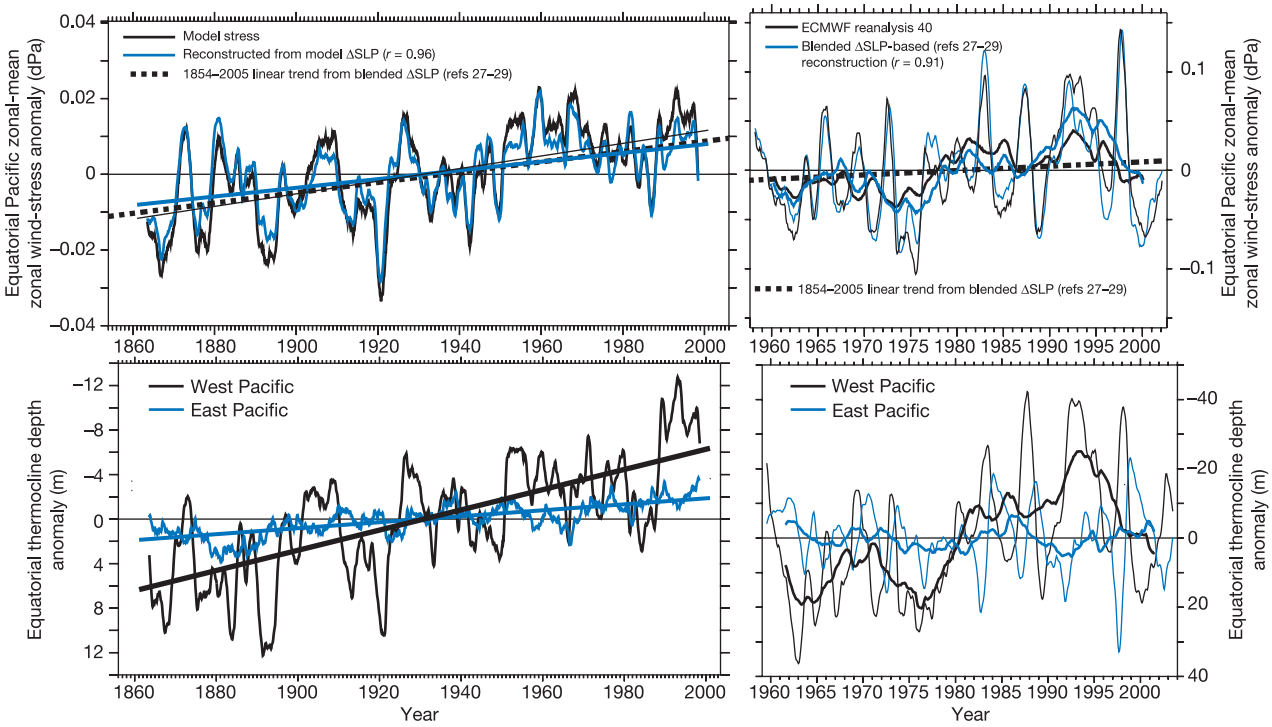

Figure 4 | Observed and modelled equatorial Pacific zonal-mean zonal wind-stress anomaly, $<\tau^x>$, and equatorial thermocline depth anomaly, Z_{tc}. Upper panels: model/observed $<\tau^x>$ and reconstruction using linear relation to ΔSLP; dashed line shows (1854–2005) trend in $<\tau^x>$ reconstructed using blended Kaplan[29]/Hadley[28]/NCEP[27] ΔSLP. Lower panels: Z_{tc} in the western (black line, 2° S–2° N, 140° E–180° E) and eastern (blue line, 2° S–2° N, 130° W–90° W) equatorial Pacific. Left panels: ensemble-mean all-forcing CM2.1 GCM experiment, showing five-year running mean. Right panels: five-year running mean (thick lines) and annual-mean (thin lines) observational estimates. Observed stress is from European Centre for Medium Range Weather Forecasting Reanalysis 40, observed Z_{tc} is from GFDL ocean data assimilation[30]. Z_{tc} is the location of the maximum vertical temperature gradient. Note different scales in each panel.

the theoretical, observed and model-produced changes in strength of atmospheric circulation suggests increased confidence in the model-projected reduction in the strength of tropical circulation during the twenty-first century[4,5,7]; on the basis of climate model simulations, this weakening may be of the order of 10% by the end of the twenty-first century[4,7].

METHODS

SLP data sets and calculations. Direct assessment of long-term changes in the strength of tropical circulation is problematic, because there have been changes in the methods used to make wind measurements at sea[23,24]. Trends in tropical winds over recent decades are ambiguous, with some studies showing a strengthening[25] and others a weakening[26]. SLP offers a proxy to recover changes in wind velocity, because of the dynamical connection between large-scale zonal gradients of SLP and zonal-mean zonal wind-stress[19]. Further, SLP measurements at sea have always been made using instruments, in contrast with measurements of surface wind, which have been instrument-based only in recent decades[23,24]. Equatorial Pacific wind-stress estimated from the zonal gradients of SLP has shown a reduction over the period 1920–90[19]. Ship-based SLP measurements[27] have been used to build global gridded data sets of monthly SLP[28,29] using knowledge of its global co-variability, and allow the exploration of changes from the mid-nineteenth century.

In this study two global reconstruction data sets of monthly SLP are used: (1) the Kaplan SLP data set[29] version 1 spanning the period 1854–1992, with data only over the ocean, and (2) the Hadley Centre SLP reconstruction[28] version 1 spanning the period 1871–1998, with data over both land and ocean. These data sets are extended into recent years using the gridded monthly ship-based SLP observations available from NOAA's National Center for Environmental Prediction (NCEP)[27]. For the analyses presented here, the monthly long-term climatology of each data set is removed to compute SLP anomalies.

Using the GCM and observed SLP data, a large-scale tropical Indo-Pacific SLP gradient (ΔSLP) is computed from the difference in SLP averaged over the central/east Pacific (160° W–80° W, 5° S–5° N) and over the Indian Ocean/west Pacific (80° E–160° E, 5° S–5° N). The index is computed with SLP anomalies from monthly climatology; positive values indicate a strengthened Indo-Pacific SLP gradient. A least-squares linear trend in ΔSLP is used as a concise metric for the long-term changes in the strength of zonal circulation. As shown in ref. 19 a large-scale SLP gradient, like ΔSLP, provides a useful proxy for the mean intensity of Pacific zonal surface winds. For the observational record of surface winds available to us (1957–2003) and for the entire climate model record (1861–2000), ΔSLP provides a useful proxy for the strength of the mean zonal circulation over the equatorial Pacific Ocean (Fig. 4).

Climate models. Global climate models (GCMs) simulate the variations of, and interactions between, various elements of the climate system (ocean, atmosphere, cryosphere and land) forced by radiatively active naturally occurring and anthropogenic gases and aerosols. Internal climate variability can be isolated from that forced by changes to atmospheric composition through ensemble experiments, in which the same model physics and forcing fields are applied to different initial conditions. The model used here is the NOAA GFDL CM2.1 GCM[16–18], which uses estimated radiative forcings over the period 1861–2000. The principal historical integration set is a five-member ensemble including estimates of natural (solar variations, volcanoes), and anthropogenic (well-mixed greenhouse gases, ozone, direct aerosol forcing and land use) sources of climate change. Two additional sets of experiments isolate the effects of each set of forcing elements, by applying only natural or anthropogenic forcing; each consists of a three-member ensemble. Statistical significance estimates are computed from a 2,000-year control integration with invariant radiative conditions from the 1860s (see Supplementary Information).

Received 27 October 2005; accepted 22 March 2006.

1. Houghton, J., *et al. Climate Change 2001: The Scientific Basis* (Cambridge Univ. Press, Cambridge, UK, 2001).
2. Rayner, N. A. *et al.* Global analyses of sea surface temperature, sea ice, and night marine air temperature since the late nineteenth century. *J. Geophys. Res.* **108**(D14), 4407, doi:10.1029/2002JD002670 (2003).
3. Knutson, T. R. *et al.* Assessment of twentieth-century regional surface temperature trends using the GFDL CM2 coupled models. *J. Clim.* (in the press).
4. Held, I. M. & Soden, B. J. Robust responses of the hydrological cycle to global warming. *J. Clim.* (in the press).
5. Knutson, T. R. & Manabe, S. Time-mean response over the tropical Pacific to increased CO_2 in a coupled ocean-atmosphere model. *J. Clim.* **8,** 2181–2199 (1995).
6. Julian, P. R. & Chervin, R. M. A study of the Southern Oscillation and the Walker Circulation. *Mon. Weath. Rev.* **106,** 1433–1451 (1978).
7. Tanaka, H. L., Ishizki, N. & Kitoh, A. Trend and interannual variability of Walker, monsoon and Hadley circulations defined by velocity potential in the upper troposphere. *Tellus A* **56,** 250–269 (2004).
8. Webster, P. J. *et al.* Monsoons: Processes, predictability, and the prospects for prediction. *J. Geophys. Res.* **103**(C7), 14451–14510 (1998).
9. Deser, C. & Wallace, J. M. Large-scale atmospheric circulation features of warm and cold episodes in the tropical Pacific. *J. Clim.* **3,** 1254–1281 (1990).
10. Cane, M. A. & Sarachik, E. S. Forced baroclinic ocean motions, Part II: The linear equatorial bounded case. *J. Mar. Res.* **35,** 395–432 (1977).
11. Barber, R. T. & Chavez, F. P. Biological consequences of El Niño. *Science* **222,** 1203–1210 (1983).
12. Trenberth, K. E., Fasullo, J. & Smith, L. Trends and variability in column integrated atmospheric water vapor. *Clim. Dyn.* **24**, doi:10.1007/s00382–005–0017–4 (2005).
13. Soden, B. J., Jackson, D. L., Ramaswamy, V., Schwarzkopf, M. D. & Huang, X. The radiative signature of upper tropospheric moistening. *Science* **310,** 841–844, doi:10.1126/science.1115602 (2005).
14. Boer, G. J. Climate change and the regulation of the surface moisture and energy budgets. *Clim. Dyn.* **8,** 225–239 (1993).
15. Allen, M. R. & Ingram, W. J. Constraints on future changes in the hydrological cycle. *Nature* **419,** 224–228 (2002).
16. Delworth, T. L. *et al.* GFDL's CM2 global coupled climate models–Part 1: Formulation and simulation characteristics. *J. Clim.* **19**(5), 643–674 (2006).
17. Wittenberg, A. T., Rosati, A., Lau, N.-C. & Ploshay, J. J. GFDL's CM2 global coupled climate models–Part 3: Tropical Pacific climate and ENSO. *J. Clim.* **19**(5), 698–722 (2006).
18. Stouffer, R. *et al.* GFDL's CM2 global coupled climate models–Part 4: Idealized climate response. *J. Clim.* **19**(5), 723–740 (2006).
19. Clarke, A. J. & Lebedev, A. Long-term changes in equatorial Pacific trade winds. *J. Clim.* **9,** 1020–1029 (1996).
20. Jin, F.-F. An equatorial ocean recharge paradigm for ENSO. Part I: Conceptual model. *J. Atmos. Sci.* **54,** 811–829 (1997).
21. Fedorov, A. V. & Philander, S. G. Is El Niño changing? *Science* **288,** 1997–2002 (2000).
22. Harrison, D. E. & Vecchi, G. A. El Niño and La Niña–Equatorial Pacific thermocline and sea surface temperature anomalies, 1986–98. *Geophys. Res. Lett.* **28,** 1051–1054 (2001).
23. Cardone, V. J., Greenwood, J. G. & Cane, M. A. On trends in historical marine wind data. *J. Clim.* **3,** 113–127 (1990).
24. Ramage, C. S. Can shipboard measurements reveal secular changes in tropical air-sea heat flux? *J. Clim. Appl. Meteorol.* **23,** 187–193 (1984).
25. Whysall, K. D. B., Cooper, N. S. & Bigg, G. R. Long-term changes in tropical Pacific surface wind field. *Nature* **327,** 216–219 (1987).
26. Harrison, D. E. Post World War II trends in tropical Pacific surface trades. *J. Clim.* **2,** 1561–1563 (1989).
27. Worley, S. J., Woodruff, S. D., Reynolds, R. W., Lubker, S. J. & Lot, N. ICOADS release 2.1 data and products. *Int. J. Climatol.* **25,** 823–842 (2005).
28. Basnett, T. & Parker, D. *Development of the Global Mean Sea Level Pressure Data Set GMSLP2* (Climate Research Technical Note 79, Hadley Centre, Met Office, Exeter, UK, 1997).
29. Kaplan, A., Kushnir, Y. & Cane, M. A. Reduced space optimal interpolation of historical marine sea level pressure. *J. Clim.* **13,** 2987–3002 (2000).
30. Derber, J. & Rosati, A. A global oceanic data assimilation system. *J. Phys. Oceanogr.* **19,** 1333–1347 (1989).

Supplementary Information is linked to the online version of the paper at www.nature.com/nature.

Acknowledgements G.A.V. was supported by the Visiting Scientist Program at the NOAA/GFDL administered by UCAR. We are grateful to the model development teams at GFDL, and thank A. E. Johansson, M. P. Vecchi, T. Knutson, T. Delworth and J. Russell for comments and suggestions.

Author Information Reprints and permissions information is available at npg.nature.com/reprintsandpermissions. The authors declare no competing financial interests. Correspondence and requests for materials should be addressed to G.A.V. (Gabriel.A.Vecchi@noaa.gov).